

AMRNET: CHIP AUGMENTATION IN AERIAL IMAGE OBJECT DETECTION

Zhiwei Wei* Chengzhen Duan* Xinghao Song Ye Tian Hongpeng Wang†

School of Computer Science and Technology, Harbin Institute of Technology (Shenzhen), China
{19S051024, 18S151541}@stu.hit.edu.cn; wanghp@hit.edu.cn

ABSTRACT

Object detection in aerial images is a challenging task due to the following reasons: (1) objects are small and dense relative to images; (2) the object scale varies in a wide range; (3) the number of object in different classes is imbalanced. Many current methods adopt cropping idea: splitting high resolution images into serials subregions (chips) and detecting on them. However, some problems such as scale variation, object sparsity, and class imbalance exist in the process of training network with chips. In this work, three augmentation methods are introduced to relieve these problems. Specifically, we propose a scale adaptive module, which dynamically adjusts chip size to balance object scale, narrowing scale variation in training. In addition, we introduce mosaic to augment datasets, relieving object sparsity problem. To balance category, we present mask resampling to paste object in chips with panoramic segmentation. Our model achieves state-of-the-art performance on two popular aerial image datasets of VisDrone and UAVDT. Remarkably, three methods can be independently applied to detectors, increasing performance steady without the sacrifice of inference efficiency.

Index Terms— Aerial images, object detection, adaptive cropping, mosaic, object resampling

1. INTRODUCTION

Object detection in aerial images has widely application, such as traffic monitoring and disaster search, due to flexible shooting view and wide receptive field. Many effective solutions have been proposed in nature scene detection[3, 4, 5]. However, aerial images have special challenges different from nature images, such as MS-COCO [6] and Pascal VOC [7] datasets. When applying the same strategy as nature images, aerial detectors usually get poor performance.

Recently, cropping-based detectors are proposed to improve performance in aerial image detection. More specifically, detectors first crop high resolution images into several subregions, denoted as chips, and detect on them. The final results is fused by the detecting of chips and original images.

Many researchers have found the significance of chips in aerial image detection. In [8], the authors splitted images uni-

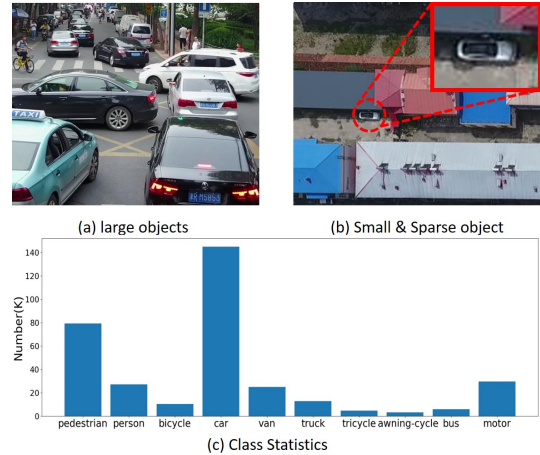


Fig. 1. Three problems in chips. (a) & (b) show the scale variation. Car size varies from small to large. (b) shows a sparse chip which contains only one car. (c) displays imbalanced quantity distribution of categories in VisDrone dataset.

formly. [9] used K-means to generate object gathering regions and trained a network to predict them. The work of [10] introduced object density maps to describe object distribution and cropped connected regions in the map. The approaches of [11] predicted potential difficult regions and detected on them.

However, there are some problems in training network with chips as shown in figure 1. First, severe scale variation exists among different chips. Second, due to the object nonuniform distribution and the shortcoming of cropping method, some chips are object sparse samples, which contains much background but less foreground. Third, chips are class imbalanced in many cases. Therefore, these chips are not good for training detectors that can fully exploit ability.

In this paper, we introduce three augmentation methods to relieve problems including scale variation, object sparsity, and class imbalance for aerial detectors based on the cropping idea. We propose an adaptive cropping module, which dynamically enlarges or reduces the chip size according to the object average scale, narrowing the scale variation. For sparse chips, we introduce mosaic [17] to augment datasets, combining multiple sparse sample subregions into a new image. To balance class, we paste object masks in chips through panoramic segmentation. We abbreviate our network as AMRNet due to three augmentation methods: adaptive cropping,

* These authors contributed equally to this work and should be considered co-first authors. † means corresponding author.

mosaic augmentation, and mask resampling.

In summary, our work contributions are as follows:

- We propose a scale adaptive cropping method, which is compatible with existing cropping method, relieving scale variation problem in training stage.
- We first introduce mosaic augmentation into aerial image detection, validating its effectiveness and alleviating object sparsity problem.
- We present the mask resampling method, pasting and adjusting masks based on local context information to relieve class imbalance problem.
- We achieve state-of-the-art object detection performance on VisDrone [1] and UAVDT [2] datasets.

2. RELATED WORK

In this section, we first review relevant aerial image detection methods, and then discuss the differences and associations among existing approaches and ours.

Subregion detection. Many researchers have detected objects on image subregions and studied how to crop images reasonably [8, 10, 11, 12, 14]. For example in [8, 14], images are partitioned uniformly into the same size chips for detection. The method in [12] proposed a dynamic zooming strategy for small object with reinforcement learning. The work of [9] generated object clusters by K-means and predicted these regions in inference. The method in [10] introduced object density maps and cropped connected regions. In [11], the authors trained a network to predict difficult regions. Above works reduce intra-sample scale variation by cropping images into chips, but not consider inter-sample scale variation.

Data augmentation. Some special data augmentation have proposed in aerial image detection. The method of [14, 15] splitted images into uniform chips to enlarge the dataset. The approach of [16] pasted small object randomly in images to improve object detection performance. In [15], the authors took advantage of semantic segmentation to paste object on road regions, avoiding the mismatch of semantic information. Motivated by [17], we introduce mosaic, combining subregions into a new image, to augment datasets and relieve object sparsity problem.

Class imbalance. Some researchers have offered some solutions for this problem. In [11], the authors used IOU (Intersection over Union) balanced sampling and balanced L1 loss to alleviate class imbalance. The work of [14] divided class into two parts and trained expert detectors separately. The approach of [15] pasted object ground truth boxes on road regions obtained from semantic segmentation. We propose mask resampling method to paste mask in images. Different from [15], we only paste instance pixel instead of the whole ground truth box to get more accurate semantic match. In addition, we consider the pasted strategies of object scale, illumination and categories.

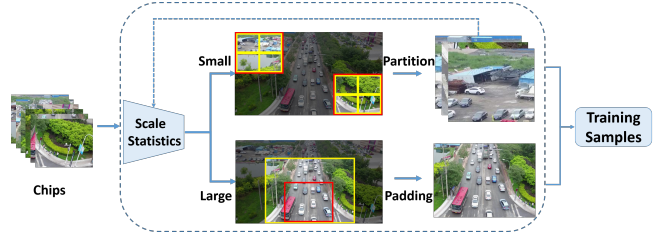


Fig. 2. Adaptive Cropping Augmentation. The red boxes represent original chips from uniform cropping. Chips will be splitted uniformly (top path) or enlarged (bottom path) to get scale adaptive chips (yellow boxes).

3. PROPOSED METHOD

Cropping images into chips and performing detection are a common method to improve performance in aerial image detection. However, some problems exist in the process of training detectors with these chips. In this section, three augmentation methods are proposed to relieve scale variation, object sparsity, and class imbalance problems. We take uniform cropping as example to describe our approaches.

3.1. Adaptive Cropping

A prominent feature of aerial images is a wide range of object scale. Due to the change of shooting angle and elevation, objects have 20 times scale variation in VisDrone [1]. Chips inherit the similar characteristic from images, which is not conducive to network training [18, 19]. Therefore, we propose a scale adaptive cropping method to relieve the inter-chip scale variation problem.

As shown in figure 2, chips from uniform cropping are fed into the scale adaption module to reconstruct the training dataset. We denote the average scale of object in chips as the chip scale. Partition or padding operation will be exploited according to scale information. If the chip scale is small, we split it uniformly into four parts. Otherwise, we enlarge it by padding pixel from original images. Chips generated from partition operation repeat the process unless it comes from padding operation or exceeds maximum iteration number.

Above processes change the coverage proportion between objects and chips. When all chips resize to a fixed resolution in training, objects in different chips are transformed into a similar scale range. We limit the maximum number of partition to avoid creating too many small chips. The detailed implementation is illustrated in algorithm 1. For each chip, we count the average scale of object in chips. Ideal and current scaling factor are calculated according to the expect scale parameter and the training resolution. Partition or padding is exploited to narrow the difference of two factors.

3.2. Mosaic Augmentation

Some chips have less foreground information, which leads to the low efficiency of network training. About one fifth chips are sparse samples which contain less three objects when we

Algorithm 1 Adaptive cropping

Input: list of chip box $B = \{b_1, \dots, b_n\}$. dict mapping chips to the number times of partition operation $I = \{b_1 : 0, \dots, b_n : 0\}$. expect scale S . training resolution I_w, I_h . maximum partition number $maxPart$.

Output: list of adaptive chip box C

```
1:  $C \leftarrow \{\}$ 
2: while  $B \neq \text{empty}$  do
3:   for  $b_i$  in  $B$  do
4:      $B \leftarrow B - b_i$ 
5:      $avg_{obj} \leftarrow \text{getObjAvgScale}(b_i)$ 
6:      $cw, ch \leftarrow \text{getBoxSize}(b_i)$ 
7:      $\triangleright$  Calculate ideal and current zoom factor
8:      $f_{cur}, f_{ideal} \leftarrow \min(\frac{I_w}{c_w}, \frac{I_h}{c_h}), \frac{S}{avg_{obj}}$ 
9:     if  $f_{ideal} > f_{cur}$  then
10:       $\triangleright$  Do partition operation
11:       $num \leftarrow I[b_i]$ 
12:      if  $num \geq maxPart$  then
13:         $C \leftarrow C \cup b_i$ 
14:      else
15:         $C_i \leftarrow \text{partition}(b_i)$ 
16:         $B \leftarrow B \cup C_i$ 
17:         $I[C_i] \leftarrow I[b_i] + 1$ 
18:      end if
19:    else
20:       $\triangleright$  Do padding operation
21:       $C_i \leftarrow \text{padding}(b_i)$ 
22:       $C \leftarrow C \cup C_i$ 
23:    end if
24:  end for
25: end while
```

split images into six parts uniformly in VisDrone [1]. Thus, we introduce mosaic [17] to solve the problem.

As shown in figure 3, we crop out the region of interest (ROI) containing foreground from sparse samples, and combine multiple regions into a new image. To avoid intra-chip scale variation caused by the too small or too large object in ROI, we first zoom in/out chips and then use sliding windows to choose appropriate regions where objects are in a reasonable scale range. f_{ideal} in algorithm 1 is adopted as the zoom factor. We extend the idea to all training samples to augment the dataset. For general samples, we not rescale them and directly choose appropriate regions because they contain more objects than that in sparse samples.

Comparing with original images, objects in mosaic have more complicate background, which helps to detect objects in different context. For example, mosaic augmentation relieve similar background problem in UAVDT [2], where images have similar semantic information because they come from series adjacent video frames.

3.3. Mask Resampling

Another notable problem in aerial datasets is class imbalance. For example, the number of cars is over 30 times than that of

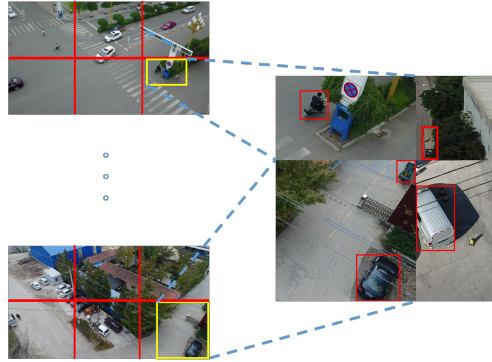


Fig. 3. Mosaci augmentation. Some chips from uniform cropping are object sparse. The subregions of sparse samples are combined into a mosaic image.

tricycles in VisDrone [1] dataset. In order to alleviate class imbalance problem, mask reasmping is proposed. We create a mask pool and pasted (road) regions by panoramic segmentation, and paste masks into chips. We also consider pasted strategies for mask category, scale and lumination.

To build a mask pool, images are fed into a COCO [6] pretrained panoramic segmentation network to get object instance masks. If the IOU of mask and ground truth box (GT) is greater than a certain threshold, the GT category will be assigned to the mask.

To ensure semantic correctness, we only collect road masks generated by segmentation to construct pasted regions. Pasted positions are randomly determined from road regions. We choose the object mask which category is compatible with the nearest object from pasted position. For example, compatible categories of van includes truck, bus. Because it is reasonable for these objects appear in a local region. The scale of the pasted object P can be calculated by a simple linear function according to the neighbour object N.

$$S_p = \frac{S_{pcls}}{S_{ncls}} * S_n \quad (1)$$
$$\overline{S_{cls}} = \frac{1}{m} \sum_{i=1}^m S_{cls}^i$$

where S_p, S_n is scale of the pasted object and the neighbour object, $\overline{S_{cls}}$ is the class average scale corresponding the class of object i. S_{cls}^i is the class average scale. We adjust the pasted mask lumination closed to that of the neighbour object in the hsv color space before pasting.

4. EXPERIMENT

4.1. Implementation Details

We use average precision (AP) as evaluation metric to validate our methods in two public datasets: VisDrone [1] and UAVDT [2]. Unless specified, we use retinaNet [4] as object detector and set input resolution as $800 \times 1,500$. Images are uniformly cropped into 6 and 4 chips as baseline on VisDrone [1] and UAVDT [2]. We use three scales 1,000, 1,500,

Table 1. Quantitative results for VisDrone dataset. The ★ denotes the multi-scale inference.

Mehod	Backbone	AP	AP_s	AP_m	AP_l
ClustDet[9]	ResNet50	26.7	17.6	38.9	51.4
ClustDet[9]	ResNet101	26.7	17.2	39.3	54.9
ClustDet[9]	ResXt101	28.4	19.1	40.8	54.4
DMNet[10]	ResNet50	28.2	19.9	39.6	55.8
DMNet[10]	ResNet101	28.5	20.0	39.7	57.1
DMNet[10]	ResXt101	29.4	21.6	41	56.9
AMRNet	ResNet50	31.7	23.0	43.4	58.1
AMRNet	ResNet101	31.7	22.9	43.4	59.5
AMRNet	ResXt101	32.1	23.2	43.9	60.5
ClustDet[9]★	ResXt101	32.4	-	-	-
AMRNet★	ResXt101	36.1	29.0	45.5	60.9

Table 2. Quantitative results for UAVDT dataset

Mehod	Backbone	AP	AP_s	AP_m	AP_l
ClusDet[9]	ResNet50	13.7	9.1	25.1	31.2
DMNet[10]	ResNet50	14.7	9.3	26.2	35.2
HFEA[11]	ResNet50	15.1	-	-	-
Baseline	ResNet50	15.2	9.4	26.3	36.8
Base+Mosaic	ResNet50	16.8	10.7	29.8	31.8
AMRNet	ResNet50	18.2	10.3	31.3	33.5

2,000 in multiple scale testing. Detector is trained for 12 and 6 epochs respectively with a batch size of 2. On VisDrone [1] dataset, learning rate sets 0.01 and decreases 0.1 times after the 8th and 11th rounds. On UAVDT [2] dataset, learning rate sets 0.005 and decreases 0.1 times after 4th and 5th rounds. For two datasets, the expect scale parameter in adaptive cropping is 100 and 60 with most one partition operation. The reason we set the parameter to twice the average scale of objects is that in inference stage, chips are scaled double on average. Object scale in mosaic limits over 50 and 30. The number of mosaic is 20k whenever not specified. In mask resampling, we paste all categories except the car class.

4.2. Quantitative Results

For fair comparisons, we train the network under the same configuration with [10] in two datasets. Table 1 shows the results on VisDrone [1]. It is noted that we surpass previous best AP with only resnet 50 as backbone. We get a high boost when detectors use multi-scale testing. We think the adptive cropping module performs well in multiple scale, so the gain in multiple scale almost catch up that in single scale.

Table 2 shows the results of different methods on UAVDT [2]. Images are similar because they come from adjacent frames. We sample images with a step of five in frames and split uniformly in 2×2 chips to reconstruct the training set. Faster RCNN [3] with FPN [20] is trained on the new dataset as baseline. Baseline achieve higher AP than previous methods. We conjecture it is not nesscessary to train networks with all images due to background similarity. In addition, dataset

Table 3. Ablation experiments on VisDrone dataset. AC,MA,MR represent our three augmentation methods: adptive cropping, mosaic augmentation, mask resampling. 10K images are augmented in MA. SR denotes the sparse sample replacement with mosaic. MS indicates multiple scale testing.

	a	b	c	d	e	f	g	h	i	j	k
AC		✓					✓		✓		✓
MA			✓					✓	✓	✓	✓
MR				✓						✓	✓
SR					✓			✓			✓
MS						✓	✓				✓
	27.0	29.5	28.8	28.5	27.4	27.6	31.2	29.1	30.6	29.0	30.8

is augmented by uniform cropping to train a more powerful detector. Remarkably, mosaic augmentation boosts 1.6 points comparing with the baseline. We think mosaic augmentation, combining subregions and creating complicate images, is suitable to relieve background similarity problem. When applying all methods, we achieve 18.2 AP with the stage-of-the-art performance.

4.3. Ablation Study

We carry out ablation experiments on VisDrone [1] without fusing original images. Table 3 shows ablation results. Three methods can be independent applied to detectors and steady improve performance (column b,c,d,e). It is worth noting that the sparse replacement gains about 0.3 points even though the dataset adds 10K mosaic images for augmentation (column c&h). In addition, we find adaptive cropping performs well in multi-scale testing. Mutiple scale increases 0.6 and 1.7 points in network without/with AC module respectively (column f&g). The reason is that detectors with AC module focuses on objects in a certain scale range and multiple scale transforms objects into the scale interval. We also study the joint effect between modules. We find mask resampling increases less, only 0.2 points when it unite with mosaic augmentation (column c&j). We hypothesize mosaic images increase the number of rare class objects, avoiding too less objects for rare category, which leads the gain overlapping with mask resampling. AC and MA are the main contribution to increase AP and few gain overlapping (column i&k).

5. CONCLUSION

In this paper, we propose three augamenataion methods in aerial image detection. Adaptive cropping reduces inter-chip scale variation by adjusting the coverage proportion between objects and chips. Masoic augmentation combines multiple image subregion to augment dataset, relieving object sparsity problem. Mask resampling balances the object number of different classes by pasting instance masks. Extend results show our approaches achieve state-of-the-art performance on two popular aerial image detection datasets. All proposed methods are cost free in inference stage and easily embedded to

other detectors based on cropping idea.

6. REFERENCES

- [1] Pengfei Zhu, Longyin Wen, Xiao Bian, Haibin Ling, and Qinghua Hu, "Vision meets drones: A challenge," *arXiv preprint arXiv:1804.07437*, 2018.
- [2] Dawei Du, Yuankai Qi, Hongyang Yu, Yifan Yang, Kaiwen Duan, Guorong Li, Weigang Zhang, Qingming Huang, and Qi Tian, "The unmanned aerial vehicle benchmark: Object detection and tracking," in *Proceedings of the European Conference on Computer Vision (ECCV)*, 2018, pp. 370–386.
- [3] Shaoqing Ren, Kaiming He, Ross Girshick, and Jian Sun, "Faster r-cnn: Towards real-time object detection with region proposal networks," in *Advances in neural information processing systems*, 2015, pp. 91–99.
- [4] Tsung-Yi Lin, Priya Goyal, Ross Girshick, Kaiming He, and Piotr Dollár, "Focal loss for dense object detection," in *Proceedings of the IEEE international conference on computer vision*, 2017, pp. 2980–2988.
- [5] Zhaowei Cai and Nuno Vasconcelos, "Cascade r-cnn: Delving into high quality object detection," in *Proceedings of the IEEE conference on computer vision and pattern recognition*, 2018, pp. 6154–6162.
- [6] Tsung-Yi Lin, Michael Maire, Serge Belongie, James Hays, Pietro Perona, Deva Ramanan, Piotr Dollár, and C Lawrence Zitnick, "Microsoft coco: Common objects in context," in *European conference on computer vision*. Springer, 2014, pp. 740–755.
- [7] Mark Everingham, Luc Van Gool, Christopher KI Williams, John Winn, and Andrew Zisserman, "The pascal visual object classes (voc) challenge," *International journal of computer vision*, vol. 88, no. 2, pp. 303–338, 2010.
- [8] F Ozge Unel, Burak O Ozkalayci, and Cevahir Cigla, "The power of tiling for small object detection," in *Proceedings of the IEEE Conference on Computer Vision and Pattern Recognition Workshops*, 2019, pp. 0–0.
- [9] Fan Yang, Heng Fan, Peng Chu, Erik Blasch, and Haibin Ling, "Clustered object detection in aerial images," in *Proceedings of the IEEE International Conference on Computer Vision*, 2019, pp. 8311–8320.
- [10] Changlin Li, Taojiannan Yang, Sijie Zhu, Chen Chen, and Shanyue Guan, "Density map guided object detection in aerial images," in *Proceedings of the IEEE/CVF Conference on Computer Vision and Pattern Recognition Workshops*, 2020, pp. 190–191.
- [11] Junyi Zhang, Junying Huang, Xuankun Chen, and Dongyu Zhang, "How to fully exploit the abilities of aerial image detectors," in *Proceedings of the IEEE International Conference on Computer Vision Workshops*, 2019, pp. 0–0.
- [12] Mingfei Gao, Ruichi Yu, Ang Li, Vlad I Morariu, and Larry S Davis, "Dynamic zoom-in network for fast object detection in large images," in *Proceedings of the IEEE Conference on Computer Vision and Pattern Recognition*, 2018, pp. 6926–6935.
- [13] Yongxi Lu, Tara Javidi, and Svetlana Lazebnik, "Adaptive object detection using adjacency and zoom prediction," in *Proceedings of the IEEE Conference on Computer Vision and Pattern Recognition*, 2016, pp. 2351–2359.
- [14] Xindi Zhang, Ebroul Izquierdo, and Krishna Chandramouli, "Dense and small object detection in uav vision based on cascade network," in *Proceedings of the IEEE International Conference on Computer Vision Workshops*, 2019, pp. 0–0.
- [15] Changrui Chen, Yu Zhang, Qingxuan Lv, Shuo Wei, Xiaorui Wang, Xin Sun, and Junyu Dong, "Rrnet: A hybrid detector for object detection in drone-captured images," in *Proceedings of the IEEE International Conference on Computer Vision Workshops*, 2019, pp. 0–0.
- [16] Mate Kisantál, Zbigniew Wojna, Jakub Murawski, Jacek Naruniec, and Kyunghyun Cho, "Augmentation for small object detection," *arXiv preprint arXiv:1902.07296*, 2019.
- [17] Alexey Bochkovskiy, Chien-Yao Wang, and Hong-Yuan Mark Liao, "Yolov4: Optimal speed and accuracy of object detection," *arXiv preprint arXiv:2004.10934*, 2020.
- [18] Bharat Singh and Larry S Davis, "An analysis of scale invariance in object detection snip," in *Proceedings of the IEEE conference on computer vision and pattern recognition*, 2018, pp. 3578–3587.
- [19] Bharat Singh, Mahyar Najibi, and Larry S Davis, "Sniper: Efficient multi-scale training," in *Advances in neural information processing systems*, 2018, pp. 9310–9320.
- [20] Tsung-Yi Lin, Piotr Dollár, Ross Girshick, Kaiming He, Bharath Hariharan, and Serge Belongie, "Feature pyramid networks for object detection," in *Proceedings of the IEEE conference on computer vision and pattern recognition*, 2017, pp. 2117–2125.